Metal-Assisted Hybridization of Oligonucleotides, Evaluation of Circular 2′-*O*-Me RNA as Ligands for the TAR RNA Target

Laurence Zapata,[a] Katell Bathany,[b] Jean-Marie Schmitter,[b] and Serge Moreau*[a]

Keywords: Chelates / Cyclisation / Nucleic acids / Self-assembly / N ligands

Two complementary oligonucleotides were conjugated with terpyridine ligands at their nearby 5′- and 3′-ends. Addition of a stoichiometric amount of a transition metal (Zn^{2+}, Fe^{2+}) resulted in a large increase in the melting temperature of the duplex. The conjugation of TPY to stem-loop oligomers provided an efficient procedure for the cyclisation of the oligomer after the addition of metal ions. Such a short stem-loop oligomer was designed to target the HIV-1 TAR RNA through loop–loop interactions. The addition of Zn^{2+} ions yielded a good ligand (K_d = 30 nM) for this RNA structural element.

Introduction

RNA has a structural complexity rivaling that of proteins.[1] Many of these RNA structures present a regulatory function through interactions with either proteins or nucleic acids,[2,3] so ligands designed to target such RNA structural elements have the potential to impair the regulatory processes they mediate. Aptameric ligands obtained from in vitro selection using DNA or RNA libraries revealed that an RNA hairpin, a ubiquitous RNA motif, can bind a target RNA hairpin efficiently through the formation of a so-called kissing complex, in which further stabilization is provided by stacking interactions between the successive stems.[4,5] With the aim of designing synthetic ligands that can target RNA hairpins, we wanted to evaluate the impact of cyclic oligomers on such structures. Circular oligonucleotides have been shown to display improved nuclease resistance, and exhibit improved specificity and affinity when targeted to complementary single-stranded oligomers.[6–8] Desiring chemical modifications that may link two short complementary strands of synthetic oligomers efficiently, we chose to introduce a high-affinity, metal-chelating terpyridine ligand at either their 3′- or 5′-termini.[9] Addition of a transition metal ion (Fe^{2+}, Ni^{2+}, Zn^{2+}) to the incubation medium would lead to the chelation of the two terpyridine moieties. We report here the synthesis and the pairing properties of oligonucleotide sequences incorporating terpyridine (TPY) units. As a first step in the evaluation of circular oligomers on RNA hairpins, we report also the preliminary data concerning the use of TPY ligands to cyclize short oligomers involved in kissing-complex formation.

[a] INSERM U-386, IFR Pathologies Infectieuses, Université Victor Segalen
146 rue Léo Saignat, 33076 Bordeaux Cedex, France
[b] Institut Européen de Chimie et Biologie, FRE CNRS 2247, 16 Avenue Pey Berland, 33607 Pessac Cedex, France

Results

Duplex Formation

First we chose two complementary DNA sequences to evaluate the contribution of the metallic bridge towards the stabilization of the strand association. This process was studied by UV thermal denaturation experiments using various strand combinations.

The terpyridine moieties were linked to the 3′- or 5′-end of oligodeoxynucleotides through phosphoramidite chemistry. The synthesis of the phosphoramidite conjugate of TPY **5** is shown in Figure 1; it follows a simple synthetic route proposed by Daniher.[10] Serinol (**1**), which mimics the spacing between the 3′- and 5′-positions of a DNA backbone, was coupled to the terpyridine acid derivative[11] **2** using PyBOP as the activating reagent.[12] The phosphoramidite **5** was obtained as a mixture of stereoisomers that were used in the solid-phase DNA synthesis. A universal support was used for the incorporation of **5** at the 3′-terminus.[13] All modified oligomers exhibited their expected ions in MALDI-TOF analyses.

The ability of the TPY ligand to crosslink two complementary DNA strands (Scheme 1) was deduced from the various thermal denaturation experiments reported in Table 1. Addition of 1 equiv. of Zn^{2+} ions to the TPY-containing duplex IV resulted in a large increase in T_m (ΔT_m = +27 °C) in comparison with that of the unmodified duplex I in HEPES buffer (10 mM HEPES pH = 7, 50 mM NaCl, 3 mM $MgCl_2$). The observed value of T_m (67 °C) was close to the one observed for oligomer V (69 °C) in which the

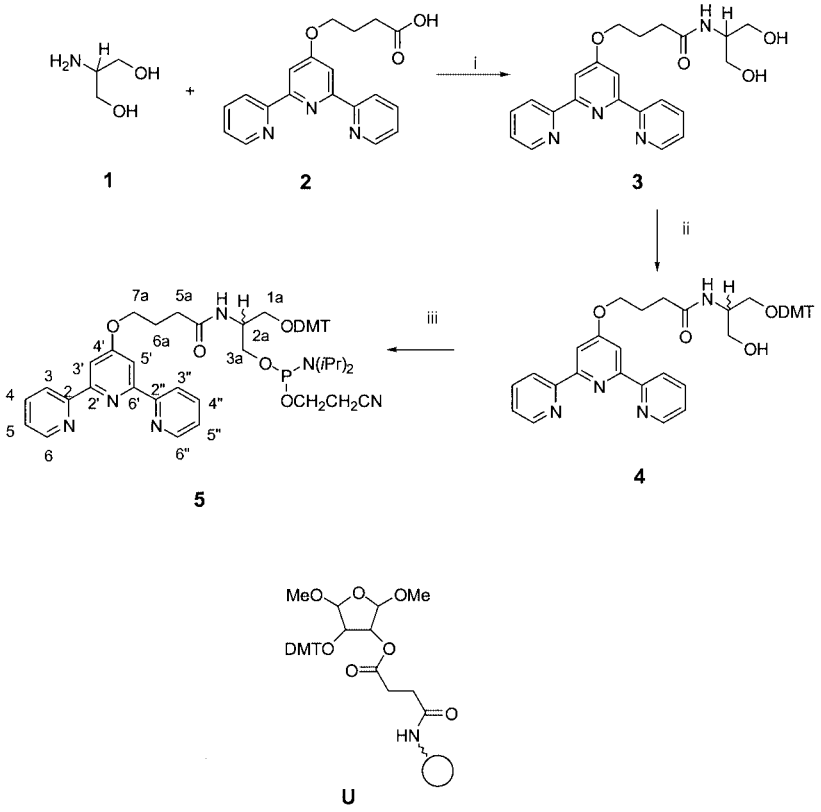

Figure 1. Synthetic pathway to compound **3** and its phosphoramidite derivative **5**; i) PyBOP, OBT, Et*i*Pr$_2$N, DMF, 65 °C, yield 55%; ii) pyridine, Et$_3$N, DMTCl, yield 58%; iii) 1,2-dichloroethane, Et*i*Pr$_2$N, 2-cyanoethyl *N*,*N*-diisopropylchlorophosphoramidite, yield 60%; U is the universal support (Glen Research) used for 3′-modified oligomers (see Exp. Sect.)

	Duplexes sequences
I	5′ TCTTTGAGGTTTA 3′ 3′ AGAAACTCCAAAT 5′
II	5′ TCTTTGAGGTTTA**4** 3′ 3′ AGAAACTCCAAAT 5′
III	5′ TCTTTGAGGTTTA 3′ 3′ AGAAACTCCAAAT**4** 5′
IV	5′ TCTTTGAGGTTTA**4** 3′ 3′ AGAAACTCCAAAT**4** 5′
V	5′ TCTTTGAGGTTTA(EG)6TAAACCTCAAAGA 3′

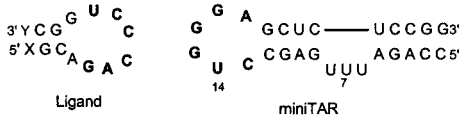

Scheme 1. Sequences of the duplexes used in the melting temperature experiments; the sketch represents the synthetic ligand (2′-*O*-methyl backbone) and the target RNA strand leading to kissing-complex formation (complementary nucleotides in the loops are in bold)

complementary strands are linked through a hexaethylene glycol bridge (Table 1). As can be deduced from the data observed for duplexes II and III, the presence of two nearby TPY ligands is a prerequisite for the stabilization through added metal ions, since no increase in stability was observed for mono-TPY-modified duplexes. When a large excess of the free ligand **2**, which acts as a high-affinity transition metal chelator, was added to the incubation buffer, the T_m for duplex IV fell to 52 °C; minor variations were exhibited by the other duplexes under these conditions.

The absorption spectrum of the free ligand **2** showed the characteristic absorption bands of the aromatic pyridyl system at 235 and 274 nm. Upon addition of Zn^{2+}, new bands at 308 and 321 nm appeared with three isosbestic points (Figure 2, top). A titration experiment was then conducted on the metal-free duplex IV monitoring the intensity of the band at 321 nm (Figure 2, bottom), which indicated a stoichiometry of one Zn^{2+} ion per duplex (i.e., two TPY units per metal ion). A similar experiment was conducted with Fe^{2+} ions and led to the same conclusion (data not shown). A mass spectrometric analysis of duplex IV was performed both in the absence and presence of a stoichiometric amount of Fe^{2+} ions. Only the metallated solution displayed peaks of a dimeric complex IV,Fe^{2+} (*m*/*z* calcd. for $[M - H]^-$: 8899.0; found 8896.9), in addition to its mono-metalated and non-metalated strands. As expected, we did not observe dimeric complexes from other strand combinations (Figure 3).

Table 1. Effect of terpyridine substituents on values of T_m [°C] of oligonucleotide complexes; all compounds are oligodeoxyribonucleotides; oligomer concentrations are 0.5 μM; melting temperature (mean values from at least three experiments) T_m (±0.5 °C); abbreviations: **2** designates the ligand **2** (Figure 1) linked through a phophodiester bond

Duplexes	10mM HEPES, 50 mM NaCl, 3 mM $MgCl_2$		10 mM HEPES			
	Zn^{2+} (1 equiv.[a])	Ligand **2** (100 equiv.[a])	Zn^{2+} (1 equiv.[a])	EDTA (200 μM)	Ligand **2** (100 equiv.[a])	Ni^{2+} (50 equiv.[a])
I	40.0	40.0	19.6	19.8	19.7	20.7
II	40.0	43.3	23.1	22.4	24.8	n.d.
III	42.0	43.5	23.8	22.0	24.2	n.d.
IV	67.0	52.0	43.0	25.5	28.3	29.0
V	69.0	70	53.0	48.5	n.d.	n.d.

[a] equiv. = equivalents; refers to duplex concentration.

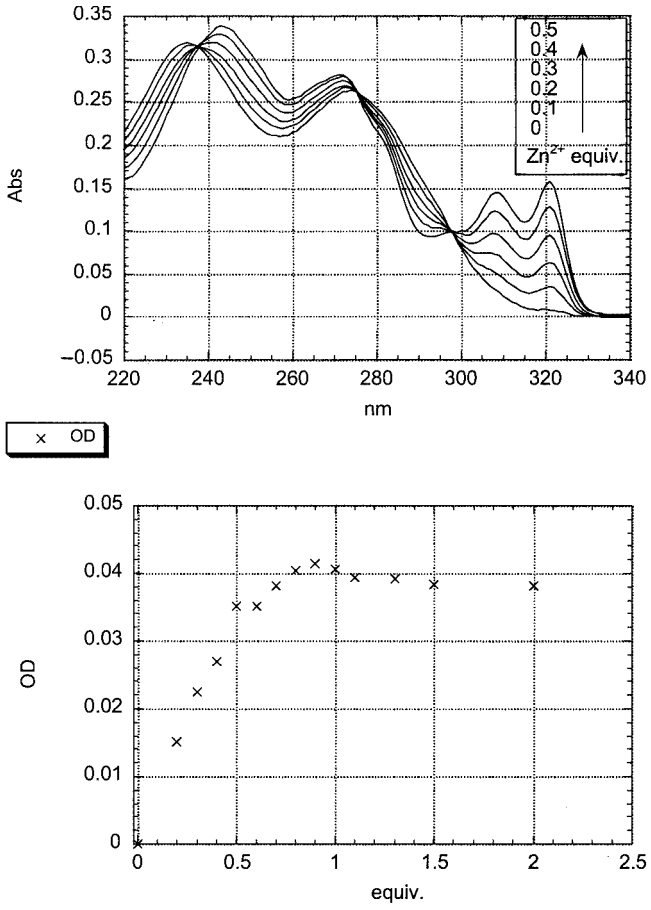

Figure 2. Top: UV absorption spectrum of ligand **2** (10^{-5} M in water) with increasing concentration of $ZnCl_2$ (Zn/TPY ratio from 0 to 0.5); complex formation was detected at λ_{max} = 321 and 308 nm; bottom: titration experiment; variation of the absorbance at 321 nm as a function of added $ZnCl_2$; equiv. (= equivalents) refers to the duplex concentration

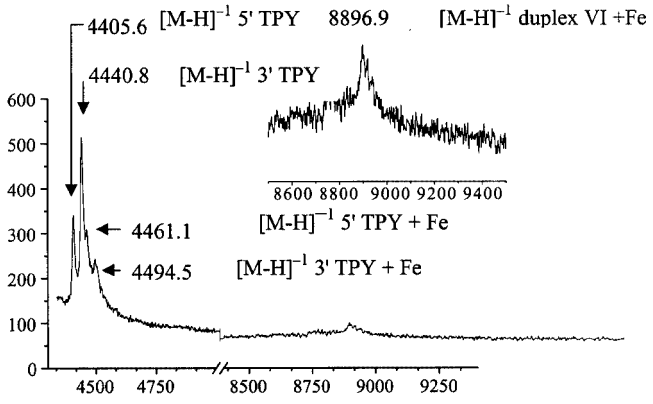

Figure 3. MALDI-ToF spectrum of the preformed duplex VI with a stoichiometric amount of Fe^{2+} ions

It must be mentioned that the high affinity of TPY ligands for transition metals resulted in complex formation from traces of metal ions contained in buffer solutions, even when they had been pretreated with a chelating resin (Chelex from Sigma). As a result, non-metallated species can be observed quantitatively only at oligomer concentrations higher than 0.5 μM or in solutions of buffers previously treated with EDTA at 200 μM (for affinity data of EDTA and iminodiacetic acids—the chelating group of Chelex—see ref.[14]). In order to analyse carefully the contributions of metallic species to the ligation of duplexes, we chose to use a low-salt-containing buffer (10 mM HEPES, pH = 7). As expected, the addition of 1 equiv. of Zn^{2+} ions per duplex strand led to an increase in the value of T_m of 23.4 °C (compare duplexes I and IV, Table 1). The use of EDTA buffer (200 μM EDTA in 10 mM HEPES) led to lower values of T_m, with the exception of the unmodified duplex I. Unmetalated bis(terpyridine) ligands, however, contribute a slight increase in the stability of the duplex (+ 5.7 °C).

The addition of a large excess of transition metal ion (Ni^{2+}, Table 1) destabilised the duplexes, as is expected from the formation of mono(terpyridine)nickel entities.[15] Thus, molecular mechanisms that are able to prevent the formation of a metallic bridge between the two TPY ligands—such as the addition of a large excess of a metal scavenger or transition metal—removes the stabilizing contribution that the two ligands bring to the duplex. Whereas the stability of a hairpin is independent of concentration, association of the TPY oligomers increases with increasing oligomer concentration, as is characteristic for bimolecular systems. Values of T_m for the complex are 43 and 54 °C at oligomer concentrations of 0.5 and 2.0 μM, respectively.

Kissing-Complex Formation

This efficient mechanism of duplex closure prompted us to evaluate the ability of such ligands to improve the stability of short stem-loop oligomers through cyclisation. It has been shown that transactivation of the transcription of the HIV-1 genome requires binding of the viral protein Tat to a structured RNA segment called the transactivation-responsive element (TAR).[16] This TAR RNA constitutes a target for artificial control of the replication of HIV-1. A small stem-loop oligomer was designed to target this TAR RNA hairpin (Scheme 1). The sequence was chosen according to studies that have identified key determinants for the loop−loop interaction. We chose to use a 2′-OMe RNA backbone since recent data have shown that RNA aptamer sequences can be changed to incorporate 2′-OMe backbones and still maintain their affinities for the target.[17] The various synthetic 2′-OMe hairpins were checked for their stability by thermal denaturation experiments, and then their affinity for a synthetic TAR RNA was evaluated both by thermal denaturation experiments and by Surface Plasmon Resonance (SPR) spectroscopy. This latter technique is used to follow, in real time, the interaction between one molecule in a continuous flow and another that has been immobilized.[18] The synthetic TAR RNA sequence was chosen according to literature data suggesting that a 27-nt-long oligomer (miniTAR) consisting of the upper part of TAR is the minimal domain necessary for responsiveness in vivo.[19] This synthetic RNA oligomer was conjugated at its 3′-end to biotin in order to immobilize it on streptavidin-coated sensor chips. The values determined for T_m and SPR data are shown in Table 2.

Table 2. Data for complex formation between the designed ligand and a minimum TAR RNA sequence. Legend: *n* = no ligand; **3** = ligand **3**; T_m = melting temperatures (average of at least three experiments (± 0.5 °C). K_d (BIAcore) were calculated as k_{off}/k_{on}. Values and errors of K_d are the average and standard deviation of at least three different experiments at different concentrations at 20 μL/min rate and 23 °C. (see Exp. Sect.)

Duplex sequences[a]		T_m [°C]	T_m complex [°C]	K_d BIAcore [nM]
VI	X = *n*			
	Y = *n*	49.0	45.0	51.0 ± 20
VII	X = **3**			
	Y = *n*	56.0	43.0	60 ± 18
VIII	X = *n*			
	Y = **3**	55.0	43.0	72 ± 17
IX	X = **3**			
	Y = **3**	66.0	50.0	30 ± 7
X	X = A			
	Y = U	57.5	51.0	21 ± 8

[a] 10 mM Hepes, 50 mM NaCl, 3 mM $MgCl_2$, Zn^{2+} (1 equiv.); equiv. = equivalents; refers to duplex concentration.

Melting temperature experiments demonstrate the efficiency of the stabilization of oligomer IX through the addition of 1 equiv. of metal ions (Zn^{2+}) per oligomer. An increase of 17 °C in T_m was observed between the unmodified hairpin VI and the bis(terpyridine) derivative IX (Table 2), suggesting that a cyclisation process occurred between the two TPY ligands. The mono(terpyridine) derivative exhibited a lower, but significant, increase in T_m, which might be related to the electrostatic effects brought about by the complexed double-charged metal ion (ΔT_m = +6 and +7 °C). Hairpin X, which incorporates an additional AU base pair, melted at 57.5 °C, which is 8.5 °C lower than that of IX.

Complexes with the target RNA (miniTAR) were first studied by UV thermal denaturation experiments. The melting profiles obtained from such mixtures should display three transitions corresponding to fusion of the complex, the synthetic hairpin, and the miniTAR target, respectively. The experimental data (Figure 4) displayed two transitions; this behaviour has been observed previously, and thus the lowest transition is assigned to the complex and the higher one to the overlap of the denaturing signals of the fusion of the target and the synthetic hairpin.[20] Only the lowest melting transitions, corresponding to the dissociation of the complex, are reported in Table 2. The cyclisation of hairpin IX by Zn^{2+} ions resulted in a clear increase in melting temperature of its complex with miniTAR. In that example, its T_m reached the value observed for the hairpin X, which includes the additional AU pair. The specificity of the complex was maintained, since melting experiments displayed that using a mutated target (nucleotides U7 and U14 mutated for C) failed to result in the formation of a complex.

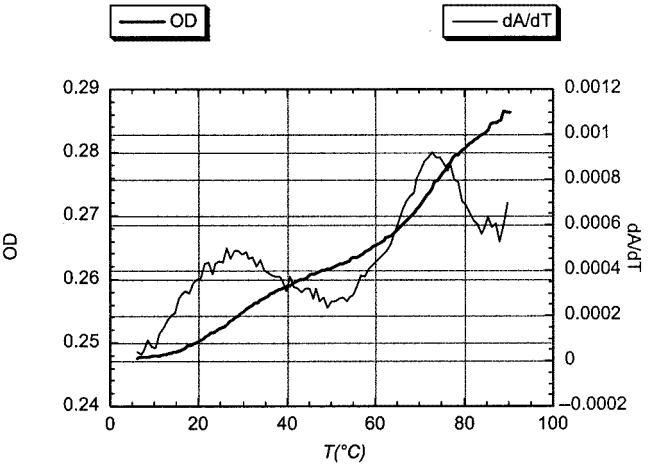

Figure 4. UV-monitored melting transition of synthetic hairpin IV−miniTAR complex; experiments were performed with 0.5 μM of each oligomer in 10 mM HEPES buffer (pH = 7.3) containing 50 mM NaCl and 0.3 mM $MgCl_2$; absorption curve in bold line and derivative in light line

SPR experiments were then performed. Sensorgrams obtained from the injection of the various hairpins to the immobilized biotinylated miniTAR allowed the values of the k_{on} and k_{off} rate constants—and therefore the values of K_d of the complexes—to be determined. (Figure 5 and Table 3). These kinetic parameters were determined by assuming a pseudo-first-order kinetic model according to Equations (1) and (2) (Exp. Sect.). Hairpins were pretreated with 1 equiv. of Zn^{2+} before injection on the sensor-chip-

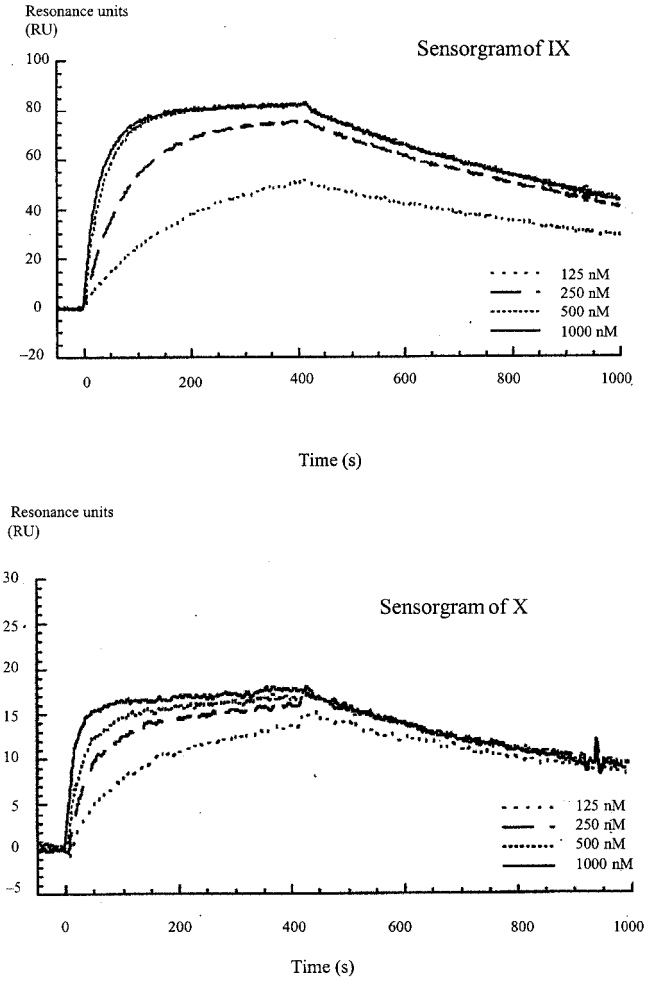

Figure 5. Sensorgrams of hairpins IX and X complexed with miniTAR; increasing concentrations of IX or X as indicated by the arrows were injected on a miniTAR-functionalized sensor chip; elementary rate constants k_{on} and k_{off} for bimolecular complex formation were deduced from direct fitting of these plots according to Equations (1) and (2) (Exp. Sect.)

immobilized target. The best ligand was obtained with the three-base-paired stem hairpin X, which displayed affinity (K_d = 21 nM) slightly lower than the one observed for the selected RNA aptamer for the same target (K_d = 6 nM). The cyclization, however, of the hairpin through the metallated terpyridine bridge clearly enhances complex stability, which is revealed by its better affinity to the ligand than that of the unmodified parent hairpin VI or the monoterpyridines VII and VIII.

Discussion

The stabilization brought by the coordination of the two TPY units upon the addition of transition metal ions is close to the strength of a covalent link. The association constant reported[15] for the bis(terpyridine)Fe^{2+} complex is as high as $10^{20.9}$. The system, however, differs in response to changes in concentration as is expected for a bimolecular process. Thus, the metal−ligand coordination is clearly a reversible process. Metal-mediated interstrand binding has recently been reported for the conception of new base pairs, revealing a cooperative binding with stabilization close to that of a base pair upon addition of Cu^{2+} ions.[21−23]

In the absence of metal ions, we observed a slight stabilisation brought by the TPY ligand in both buffer conditions (Table 1). We hypothesize that this stabilisation arises from the stacking and hydrophobic contributions of the aromatic pyridyl units at duplexes' ends. This hydrophobic contribution seems to increase with the addition of the free TPY ligand **3**. Similar observations have been reported for cholesteryl-modified oligomers.[24,25]

When applied to loop oligomers, our approach led to the formation of cyclic species. Hairpins with stems as short as two base pairs can be stabilized efficiently through crosslinking of nearby TPY ligands upon addition of one equivalent of Zn^{2+} ions. When this stabilized hairpin was used as a ligand for an RNA target, we detected the formation of a complex both by UV-monitored thermal denaturation and SPR experiments. As previously reported, there is no perfect correlation between the thermal stability of the hairpin and the stability of the complex formed with miniTAR, although the continuous stacking between the stems is necessary.[20] Although stacking interactions are not involved in the stabilization of the hairpin, they allow the formation of a complex with stability constants close to those of selected aptamers. Thus, the metallic bridge next to the last base pair of the stem does not disturb the continuous stacking between the miniTAR and hairpin stems through the loop−loop interaction.

Conclusion

This strategy may allow the synthesis of circular oligonucleotides, which remains a challenging task.[26] Thus, dumbbell oligonucleotides can be obtained easily in high yield and used as double-stranded decoys for transcription

Table 3. Equilibrium and rate constants for the various complexes formed with miniTAR

OLIGOS		k_{off}	±	k_{on}	±	K_d [nM]	±
VI		1.62×10^{-3}	4×10^{-4}	2.69×10^{4}	0.75×10^{4}	51	20
X		1.1×10^{-3}	2×10^{-4}	5.38×10^{4}	1.32×10^{4}	21	8
VIII	0.5 equiv. Zn^{2+}	1.06×10^{-3}	4.5×10^{-5}	1.47×10^{4}	2.9×10^{3}	72	17
VII		8.62×10^{-4}	7.9×10^{-5}	1.44×10^{4}	3.1×10^{3}	60	18
IX		0.99×10^{-3}	3.4×10^{-5}	3.26×10^{4}	0.69×10^{4}	30.4	7

factors or RNaseH.[27,28] The high affinity constant exhibited by the terpyridines for various metal ions might allow that such a cyclisation process occurs in vivo. Physiological metal ions, such as iron or zinc, could be recruited to mediate such a process.[29,30]

Experimental Section

General: Thin layer chromatography was performed on Merck silica gel $60F_{254}$ aluminium-backed plates. Flash chromatography refers to column chromatography performed with a BIOTAGE system. NMR spectra were recorded with a Bruker AC200 spectrometer working at 200 MHz for ^1H, 50.32 MHz for ^{13}C, and 81.02 MHz for ^{31}P. The chemical shifts are expressed in ppm using TMS as internal standard (for ^1H and ^{13}C data) and 85% H_3PO_4 as external standard (^{31}P data). Mass spectra measurements were performed with a MALDI-ToF mass spectrometer (Reflex III, Bruker) operated in the linear mode for negative-ion detection, using a mixture of oligonucleotides $d(T_{12}) - d(T_{18})$ (Sigma) for external calibration. A special sample preparation technique was designed to analyse the complexes. The stainless-steel target was first covered with a thin layer of matrix [0.5 μL of 2,4,6-trihydroxyacetophenone (THAP), 10 mg/mL in acetone], and this layer was washed with a saturated EDTA solution (2 × 1 μL) and water (2 × 1 μL). The oligonucleotides (0.5 μL of 20 μM solutions in water; alone or precomplexed with Fe^{2+}) were then deposited on this matrix layer and allowed to dry. The final preparation step was the application of a second layer of matrix [0.5 μL of a 1:1 solution of THAP (30 mg/mL in ethanol) and 100 mM aqueous ammonium citrate] and drying at room temperature.

4-(2,2′:6′,2"-Terpyridin-4′yl-oxy)butyric Acid (Potassium Salt) (2): Potassium hydroxide (7 g) was crushed and kept under vacuum 30 min before utilisation. KOH was dissolved in anhydrous DMSO (90 mL) and was stirred for 30 min at 65 °C. 4-Hydroxybutyric acid (4.8 g, 0.046 mmol) was added, the mixture was stirred at 65 °C to effect complete dissolution, and then 4′-chloro-2,2′:6′,2′′-terpyridine (7.46 mmol, 2 g,) was added. The reaction mixture was stirred overnight at 65 °C. The product was concentrated to dryness and then dissolved in water (100 mL). The pH was adjusted to 6−7 with concentrated HCl, causing a white precipitate to form. After filtration, this precipitate was dissolved in CH_2Cl_2/MeOH (2:1), concentrated, and recrystallised from acetone at 4 °C, to yield **2** (1.9 g, 70%). ^1H NMR (200 MHz, [D$_6$]DMSO): δ = 2.02 (tt, ^3J = 6, J = 7 Hz, 2 H, 3-H), 2.44 (t, ^3J = 7 Hz, 2 H, 2-H), 4.23 (t, ^3J = 6 Hz, 2 H, 4-H), 7.47 (ddd, ^4J = 1, ^3J = 5.6, ^3J = 7.4 Hz, 2 H, 5-H and 5′′-H Tpy), 7.93 (s, 2 H, 3′-H and 5′-H Tpy), 7.97 (dt, ^4J = 1.5, ^3J = 7.4 Hz, 2 × 4-H and 4′′-H Tpy), 8.57 (dd, ^4J = 1.5, ^3J = 5.6 Hz, 2 H, 6-H and 6′′-H Tpy), 8.70 (dd, ^4J = 1, ^3J = 7.4 Hz, 2 H, 3-H and 3′′-H Tpy) ppm. ^{13}C NMR (50.32 MHz, [D$_6$]DMSO): δ = 0.06 (C-3), 30.1 (C-2), 67.2 (C-4), 106.7 (C-3′ and C-5′ Tpy), 120.8 (C-5 and C-5′′ Tpy), 124.5 (C-3 and C-3′′ Tpy), 137.3 (C-4 and C-4′′ Tpy), 149.2 (C-6 and C-6′′ Tpy), 154.8 (C-2 and C-2′′ Tpy), 156.6 (C-2′ and C-6′ Tpy), 166.6 (C-4′ Tpy), 174.1(C-1) ppm.

***N*-[2-Hydroxy-1-(hydroxymethyl)ethyl]-4-(2,2′;6′,2′′-terpyridin-4′-yloxy)butyramide (3):** 1-Hydroxybenzotriazole (37 mg, 1 equiv.), PyBOP (351 mg, 2.5 equiv.), ethyldiisopropylamine (235 μL, 5 equiv.) and serinol (50 mg, 2 equiv.) were added to a solution of **2** (100 mg, 0.27 mmol) in dry DMF (5 mL). The reaction mixture was stirred for 4 h at 60 °C. After evaporation of the solvent, the crude product was dissolved in CH_2Cl_2/MeOH (2:1). The organic phase was washed with water, dried (Na_2SO_4), and concentrated. The product was purified by flash chromatography eluting with 10% MeOH/CH_2Cl_2 to yield **3** (60 mg, 54%). ^1H NMR (200 MHz, [D$_6$]DMSO): δ = 2.02 (m, 2 H, 6-H), 2.33 (m, 2 H, 7-H), 3.37 (d, ^3J = 7 Hz, 4 H, 1-H and 3-H), 3.73 (m, 1 H, 2-H), 4.27 (t, ^3J = 7.4 Hz, 2 H, 5-H), 7.50 (dd, ^3J = 4.2, ^3J = 7.4 Hz, 2 H, 5-H and 5′′-H Tpy), 7.96 (s, 2 H, 3′-H and 5′-H Tpy), 7.99 (dt, ^4J = 2, ^3J = 8 Hz, 2 H, 4-H and 4′′-H Tpy), 8.60 (d, ^3J = 7.4 Hz, 2 H, 6-H and 6′′-H Tpy), 8.71 (d, ^3J = 4.2 Hz, 2 H, 3-H and 3′′-H Tpy) ppm. ^{13}C NMR (50.32 MHz, [D$_6$]DMSO): δ = 24.7 (C-6), 31.6 (C-5), 52.8 (C-2), 60.2 (C-1 and C-3), 67.5 (C-7), 106.7 (C-3′ and C-5′ Tpy), 120.8 (C-5 and C-5′′ Tpy), 124.5 (C-3 and C-3′′ Tpy), 137.4 (C-4 and C-4′′ Tpy), 149.2 (C-6 and C-6′′ Tpy), 154.8 (C-2 and C-2′′ Tpy), 156.6 (C-2′ and C-6′ Tpy), 166.7 (C-4′ Tpy), 171.5 (C-4) ppm.

***N*-[2-(4,4′-Dimethoxytrityl)1-(hydroxymethyl)ethyl]-4-(2,2′;6′,2′′-terpyridin-4′-yloxy)butyramide (4):** Compound **3** (150 mg, 0.37 mmol) was dried by three coevaporations with anhydrous pyridine and then dissolved in anhydrous pyridine (15 mL). 4,4′-Dimethoxytrityl chloride (138 mg, 1.1 equiv.) was added. The reaction mixture was stirred for 2 h at room temp. and then poured into H_2O and extracted with CH_2Cl_2/MeOH (2:1). The organic phase was dried (Na_2SO_4) and concentrated. The product was purified by flash chromatography with a gradient of MeOH/CH_2Cl_2 (from 0 to 4% in MeOH), containing TEA (1%). Yield: 105 mg (40%). ^1H NMR (200 MHz, $CDCl_3$): δ = 2.17 (m, 2 H, 6-H), 2.38 (m, 2 H, 7-H), 3.12 (ddd, ^3J = 4, ^3J = 7.3, ^3J = 7.3 Hz, 1 H, 2-H), 3.29 (m, 2 H, 3-H), 3.74 (m, 8 H, CH_3 DMT and 1-H), 4.24 (t, ^3J = 6.5 Hz, 2 H, 5-H), 6.79 (d, ^3J = 7.3 Hz, 4 H, Ar DMT), 7.16−7.39 (m, 11 H, 5-H and 5′′-H Tpy and Ar DMT), 7.82 (dt, ^4J = 2, ^3J = 6.6 Hz, 2 H, 4-H and 4′′-H Tpy), 7.98 (s, 2 H, 3′-H and 5′-H Tpy), 8.57 (d, ^3J = 8 Hz, 2 H, 6-H and 6′′-H Tpy), 8.65 (dd, ^4J < 1, ^3J = 7.7 Hz, 2 H, 3-H and 3′-H Tpy) ppm. ^{13}C NMR (50.32 MHz, $CDCl_3$): δ = 24.9 (C-6), 32.9 (C-5), 51.2 (C-2), 55.2 (CH_3 DMT), 63.1 (C-1), 63.5 (C-3), 67.2 (C-7), 86.4 (Cq DMT), 107.4 (C-3′ and C-5′ Tpy), 113.2 (C_{Ar} DMT), 121.4 (C-5 and C-5′′ Tpy), 123.8 (C-3 and C-3′′ Tpy), 126.9, 127.92, 129.9 (C_{Ar} DMT), 135.65 (Cq DMT), 136.8 (Cq DMT and C-4 and C-4′′ Tpy), 144.5 (Cq DMT), 148.9 (C-6 and C-6′′ Tpy), 156.0 (C-2 and C-2′′ Tpy), 157.1 (C-2′ and C-6′ Tpy), 158.5 (Cq DMT), 167.0 (C-4′ Tpy), 172.5 (C-10) ppm.

Compound 5: A solution of ethyldiisopropylamine (63 μL, 0.36 mmol) and 2-cyanoethyl chloro(diisopropylamido)-phosphite (32 mg, 0.13 mmol) in anhydrous dichloromethane (1 mL) was added to a solution of **4** (64 mg, 0.09 mmol) in anhydrous dichloromethane (4 mL). After 40 min at room temp., the reaction was quenched with methanol (100 μL). The crude product was purified by chromatography on alumina with 1% TEA/CH_2Cl_2 to yield **5** (48 mg, 58%). ^1H NMR (200 MHz, $CDCl_3$): δ = 1.10 (m, 12 H, CH_3 *i*Pr), 2.14 (m, 2 H, 6a-H), 2.33 (m, 2 H, 5a-H), 2.5 (t, ^3J = 7 Hz, 2 H, CH_2CN), 3.10 (m, 1 H, 2-H), 3.34−3.80 (m, 14 H, 1-H, 3-H, CH_3 DMT, CH_2OP and CH *iPr*), 4.23 (t, ^3J = 6 Hz, 2 H, 7a-H), 6.78 (d, ^3J = 8 Hz, H_{Ar} DMT), 7.15−7.37 (m, 11 H, 5-H Tpy, 5′′-H Tpy and Ar DMT), 7.82 (dt, ^4J = 3, J = 7.7 Hz, 2 H, 4-H and 4′′-H Tpy), 7.98 (s, 2 H, 3′-H and 5′-H Tpy), 8.60 (d, ^3J = 8 Hz, 2 H, 6-H and 6′′-H Tpy), 8.64 (m, 2 H, 3-H and 3′-H Tpy) ppm. ^{13}C NMR (50.32 MHz, $CDCl_3$): δ = 20.2 (CH_2CN), 24.4 and 24.6 (CH_3 *iPr*), 24.8 (C-6a), 32.6 (C-5a), 42.8 and 43.1 (CH *iPr*), 49.5 (C-2a), 55.1 (CH_3 DMT), 58.2 (CH_2OP), 61.5 (C-1a and C-3a), 67.1 (C-7a), 85.4 (Cq DMT), 107.3 (C-3′ and C-5′ Tpy), 113.1 (C_{Ar} DMT), 117.3 (CN), 121.2 (C-5 and C-5′′ Tpy), 123.8 (C-3 and C-3′′ Tpy), 126.8, 127.78, 128.07, 123.1 (C_{Ar} DMT), 135.8 (Cq DMT), 136.7 (C-4 and C-4′′ Tpy), 144.7 (Cq

DMT), 149.0 (C-6 and C-6′′ Tpy), 156.0 (C-2 and C-2′′ Tpy), 157.0 (C-2′ and C-6′ Tpy), 158.4 (Cq DMT), 166.9 (C-4′ Tpy), 171.5(C-4) ppm. ^{31}P NMR (81.02 MHz, $CDCl_3$): δ = 145.4 and 145.5 ppm.

Oligonucleotide Synthesis: All oligonucleotides were synthesized on a 0.2-μmol scale with a Millipore Expedite 9809 synthesizer using conventional β-cyanoethyl phosphoramidite chemistry (*N*-acetyl-dC phosphoramidite monomer was used to allow fast deprotection). The standard bases were dissolved in anhydrous acetonitrile (0.1 M final concentrations). The modified phosphoramidites were dissolved in anhydrous dichloromethane and coupled manually with a coupling time of 15 min. The coupling efficiency was the same as that of unmodified amidites. All oligomers were synthesized "trityl off". Standard supports were treated for 30 min with AMA (NH_4OH/methylamine, 50:50, v:v, 1 mL) at 65 °C. Universal supports (3′-modified oligomers; Glen Research; see Figure 1) were treated overnight with AMA (1 mL) at 55 °C. The crude oligonucleotides were purified by electrophoresis on denaturating polyacrylamide gels. The pure samples were desalted through reverse-phase maxi-clean cartridges (C18, Altech) (see also Table 4).

Table 4. Mass spectral analysis of modified oligomers

Oligomer sequence (5′ to 3′)	Calcd. mass	Found mass
4TAAACCTCAAAGA	4403.9	4408.4
ATTTGGAGTTTCT**4**	4439.4	4442.0
CGGUCCCAGACG**4**	4446.5	4443.7
4CGGUCCCAGACG	4415.9	4414.4
4CGGUCCCAGACG**4**	4916.6	4916.1

UV-Monitored Melting Experiments: Purified oligonucleotides (each strand 0.5 μM) were diluted in 0.5 mL of 10 mM HEPES (pH = 7.5) or 10 mM HEPES (pH = 7.5)/3 mM $MgCl_2$/50 mM NaCl. The mixture was boiled for 2 min and the hybridization was assured by low-temperature cooling of the sample. Melting experiments were performed with a Cary 1E UV/Vis spectrophotometer with a temperature controller unit. Samples were kept at 4 °C for at least 30 min and then heated from 4 to 90 °C at a rate of 0.5 °C/min. The absorbance at 260 nm was measured every 30 s. The melting temperature was determined from the maxima of the first derivative.

Surface Plasmon Resonance (SPR) Kinetic Measurements: SPR experiments were performed with a BIAcore 2000 apparatus. Biotinylated miniTAR RNA (200−300 RU) was immobilized on CM5 sensor chips coated with streptavidin according to the procedure described previously.[20] Experiments to determine binding kinetics were performed at 23 °C in a 20 mM HEPES buffer (pH = 7.3) containing 20 mM sodium acetate, 140 mM potassium acetate and 3 mM magnesium acetate. All oligonucleotide and metal ion solutions were prepared in this buffer. The oligonucleotides were injected at a flow rate of 20 μL/min. The kinetic parameters were determined assuming a pseudo-first-order model according to Equations (1) and (2), for the association and dissociation phases, respectively.

$$\frac{dR}{dt} = k_{on}C(R_{max} - R) - k_{off}R \quad (1)$$

$$\frac{dR}{dt} = -k_{off}R \quad (2)$$

Acknowledgments

We thank Dr. Jean-Jacques Toulmé for helpful discussion and E. Dausse for technical assistance with the BIAcore experiments.

[1] R. T. Batey, R. P. Rambo, J. A. Doudna, *Angew. Chem.* **1999**, *111*, 2472−2491; *Angew. Chem. Int. Ed.* **1999**, *38*, 2327−2343.
[2] J. J. Toulmé, C. Di Primo, S. Moreau, *Prog. Nucleic Acid Res. Mol. Biol.* **2001**, *69*, 1−46.
[3] Y. Tor, *Angew. Chem. Int. Ed.* **1999**, *38*, 1579−1582.
[4] C. Boiziau, E. Dausse, L. Yurchenko, J. J. Toulme, *J. Biol. Chem.* **1999**, *274*, 12730−12737.
[5] F. Ducongé, J. J. Toulmé, *RNA* **1999**, *5*, 1605−1614.
[6] E. T. Kool, *J. Am. Chem. Soc.* **1991**, *113*, 6265−6266.
[7] E. T. Kool, *Acc. Chem. Res.* **1998**, *31*, 502−510.
[8] T. H. Li, D. S. Liu, J. Chen, A. H. F. Lee, J. Y. Qi, A. S. C. Chan, *J. Am. Chem. Soc.* **2001**, *123*, 12901−12902.
[9] R. B. Martin, J. A. Lissfelt, *J. Am. Chem. Soc.* **1956**, *78*, 938−940.
[10] A. T. Daniher, J. K. Bashkin, *Chem. Commun.* **1998**, 1077−1078.
[11] G. R. Newkome, F. Cardullo, E. C. Constable, C. N. Moorefield, A. M. W. Cargil Thompson, *J. Chem. Soc., Chem. Commun.* **1993**, 925.
[12] J. Coste, D. Lenguyen, B. Castro, *Tetrahedron Lett.* **1990**, *31*, 205−208.
[13] S. Scott, P. Hardy, R. C. Sheppard, M. J. McLean, *Innovations and Perspectives in Solid Phase Synthesis, 3rd International Symposium*, **1994**, pp. 115−124.
[14] R. M. C. Dawson, D. C. Elliot, W. H. Elliot, K. M. Jones, *Data for Biochemical Research*, Oxford University Press, New York, **1986**.
[15] R. H. Holyer, C. D. Hubbard, S. F. A. Kettle, R. G. Wilkins, *Inorg. Chem.* **1966**, *5*, 622−625.
[16] J. Karn, *J. Mol. Biol.* **1999**, *293*, 235−254.
[17] F. Darfeuille, A. Arzumanov, M. J. Gait, C. Di Primo, J. J. Toulme, *Biochemistry* **2002**, *41*, 12186−12192.
[18] U. Jonsson, L. Fagerstam, B. Ivarsson, B. Johnsson, R. Karlsson, K. Lundh, S. Lofas, B. Persson, I. Ronnberg, H. Roos, S. Sjolander, R. Stahlberg, E. Stenberg, C. Urbaniczky, *BioTechniques* **1991**, *11*, 620−627.
[19] A. Jakobovits, D. H. Smith, E. B. Jakobovits, D. J. Capon, *Mol. Cell. Biol.* **1988**, *8*, 2555−2561.
[20] F. Ducongé, C. Di Primo, J. J. Toulmé, *J. Biol. Chem.* **2000**, *275*, 21287−21294.
[21] E. Meggers, P. L. Holland, W. B. Tolman, F. E. Romesberg, P. G. Schultz, *J. Am. Chem. Soc.* **2000**, *122*, 10714−10715.
[22] K. Tanaka, Y. Yamada, M. Shionoya, *J. Am. Chem. Soc.* **2002**, *124*, 8802−8803.
[23] H. Weizman, Y. Tor, *J. Am. Chem. Soc.* **2001**, *123*, 3375−3376.
[24] R. L. Letsinger, S. K. Chaturvedi, F. Farooqui, M. Salunkhe, *J. Am. Chem. Soc.* **1993**, *115*, 7535−7536.
[25] R. L. Letsinger, S. Chaturvedi, *Bioconjugate Chem.* **1998**, *9*, 826−830.
[26] E. Alazzouzi, N. Escaja, A. Grandas, E. Pedroso, *Angew. Chem. Int. Ed. Engl.* **1997**, *36*, 1506−1508.
[27] L. Aguilar, A. Hemar, A. Dautry-Varsat, M. Blumenfeld, *Antisense Nucleic Acid Drug Dev.* **1996**, *6*, 157−163.
[28] W. S. Park, N. Miyano-Kurosaki, T. Abe, K. Takai, H. Takaku, *Nucleic Acids Symp. Ser.* **1999**, *42*, 225−226.
[29] J. M. Berg, Y. Shi, *Science* **1996**, *271*, 1081−1085.
[30] A. Rolfs, M. A. Hediger, *J. Physiol.* **1999**, *518*, 1−12.

Received October 11, 2002
[O02566]